# Model of the Induction Machine including Saturation

José M. Aller , Daniel Delgado, Alexander Bueno, Julio C. Viola and José A. Restrepo
UNIVERSIDAD SIMÓN BOLÍVAR
Valle de Sartenejas, Baruta, Edo. Miranda
Caracas, Venezuela
Phone: +58 (212) 906-3735
Fax: +58 (212) 906-3720
Email: jaller@usb.ve
URL: http://www.usb.ve

## Acknowledgments

This work was supported by FONACIT-Venezuela under project 2011000970, the Dean of Research and Development Bureau of the Simón Bolívar University (GID-04) and Universidad Politécnica Salesiana - Ecuador. This work has been financed by PROMETEO project from SENESCYT-Ecuador.

## Keywords

<<Electrical machine>>, <<AC machine>>, <<Induction motor>>, <<Flux model>>, <<Modelling>>,<<Saturation>>.

## Abstract

This work proposes a model for induction machines in natural coordinates “abc”, developed considering the nonlinear characteristics of saturation. Traditionally, the models for the induction machine including this effect make use of linear transformations. However, the nonlinearity of saturation does not allow the use of these transformations, giving invalid results. Flux linkage in each phase leads to the saturation coefficient and this to the magnetic permeance. Hence, the saturation coefficient produces a new inductance in natural coordinates that considers the nonlinearity of saturation. The machine behavior is computed using a state variable model in natural coordinates described in the space vector frame. The results obtained by the proposed model give a better harmonic representation than the “dq0”models obtained by neglecting the magnetic hysteresis effect. A comparison between the proposed representation and the traditional one shows the advantages of the former.

## Introduction

Asymmetric converters used recently as main power supply for induction machines have been explored in [1, 2]. These power stages inject large amounts of zero sequence component in current and voltage. Any unbalance in the converter’s operation will result in saturation of the magnetic core, affecting the stator current waveform shape. This call for the use of models that take into account the saturation effect. The approach commonly employed in the existing literature [3, 4, 5] assumes a linear behavior, since they

employ different linear transformations, such as Clarke, Park, space vectors, symmetric components, etc. [6, 7]. These methods give a proper representation of the magnetic path for the corresponding transformed current. However, the real values of the current in natural coordinates cannot be directly obtained because the saturation is a localized in space phenomena affecting the relationship between the original currents (in "abc" coordinates) and the transformed currents.

This work proposes using a strategy similar to the one employed in the saturation analysis of synchronous machines [8, 9]. This method employs the permeance variations using the nonlinear relation between the electromotive force and the excitation current (no load test). This results in a saturation coefficient, obtained by dividing the nonlinear excitation current and its air-gap linear projection. Synchronous machines need compensating only the direct axis reactance, because the quadrature axis has a large air-gap and the saturation is not reached in that axis. This is not the case for the induction machine, because in general the air-gap is almost constant when neglecting the slot effects.

Since the flux linkage relation with electromotive force is linear, this is straightforward to get a model with these state variables. This representation allows defining the space vector for the flux linkage (since the model is linear in flux and current). The relationship between the flux linkages and currents in real machines is nonlinear, but a proper correction in the inductances compensates for the saturation effect. This correction in the inductances is done in each winding considering the flux linkage magnitude across each winding. This produces a model of the machine in original "abc" coordinates, where the inductance matrix contains the correction terms between the different winding (stator and rotor). The resulting inductance matrix is not symmetrical neither circulant [10], the decoupling (diagonalization) of the matrix cannot be attained using modal analysis with the traditional symmetric component transformation.

In this work the proposed model is compared with the space vector based models in "$dq0$" coordinates system and with results from experimental tests. The stator currents obtained with the proposed model show a closer behavior to the ones from the practical tests.

## Induction Machine Model Considering Saturation

The linear model for the induction machine, shown in figure 1, assuming sinusoidal magnetomotive force distribution in the airgap and neglecting slots effects and hysteresis, can be expressed as:

$$[\mathbf{v}] = [\mathbf{R}]\,[\mathbf{i}] + \mathrm{p}[\lambda] = [\mathbf{R}]\,[\mathbf{i}] + \mathrm{p}[[\mathbf{L}(\theta)]\,[\mathbf{i}]] \;\; ; \;\; \mathrm{p} = \frac{d}{dt} \tag{1}$$

$$T_e - T_m = \vec{\lambda}_s \times \vec{i}_s - T_m = J\,\ddot{\theta} + \rho\,\dot{\theta} \tag{2}$$

where,

$$\vec{x}_s = \sqrt{\frac{2}{3}}\left(x_{sa}(t) + x_{sb}(t)\,e^{j\frac{2\pi}{3}} + x_{sb}(t)\,e^{j\frac{4\pi}{3}}\right) \;\; ; \;\; \forall x \in \{i, \lambda\} \tag{3}$$

$$[R] = \begin{bmatrix} R_s\,[I] & [0] \\ [0] & R_r\,[I] \end{bmatrix} \;\; : \;\; [L(\theta)] = \begin{bmatrix} L_{\sigma s}\,[I] + L_{ms}\,[S] & L_{sr}\,[C(\theta)] \\ L_{sr}\,[C(\theta)]^t & L_{\sigma r}\,[I] + L_{mr}\,[S] \end{bmatrix} \tag{4}$$

$$[I] = \begin{bmatrix} 1 & 0 & 0 \\ 0 & 1 & 0 \\ 0 & 0 & 1 \end{bmatrix} \; ; \; [S] = \begin{bmatrix} 1 & -\frac{1}{2} & -\frac{1}{2} \\ -\frac{1}{2} & 1 & -\frac{1}{2} \\ -\frac{1}{2} & -\frac{1}{2} & 1 \end{bmatrix} \tag{5}$$

$$[C(\theta)] = \begin{bmatrix} \cos\theta & \cos(\theta + \frac{2\pi}{3}) & \cos(\theta + \frac{4\pi}{3}) \\ \cos(\theta + \frac{4\pi}{3}) & \cos\theta & \cos(\theta + \frac{2\pi}{3}) \\ \cos(\theta + \frac{2\pi}{3}) & \cos(\theta + \frac{4\pi}{3}) & \cos\theta \end{bmatrix} \tag{6}$$

$$[v] = \begin{bmatrix} \begin{bmatrix} v_a^s & v_b^s & v_c^s \end{bmatrix}^t \\ \begin{bmatrix} v_a^r & v_b^r & v_c^r \end{bmatrix}^t \end{bmatrix} ; [i] = \begin{bmatrix} \begin{bmatrix} i_a^s & i_b^s & i_c^s \end{bmatrix}^t \\ \begin{bmatrix} i_a^r & i_b^r & i_c^r \end{bmatrix}^t \end{bmatrix} ; [\lambda] = \begin{bmatrix} \begin{bmatrix} \lambda_a^s & \lambda_b^s & \lambda_c^s \end{bmatrix}^t \\ \begin{bmatrix} \lambda_a^r & \lambda_b^r & \lambda_c^r \end{bmatrix}^t \end{bmatrix} \tag{7}$$

 ISBN: 978-90-75815-17-7 and 978-1-4799-0114-2 

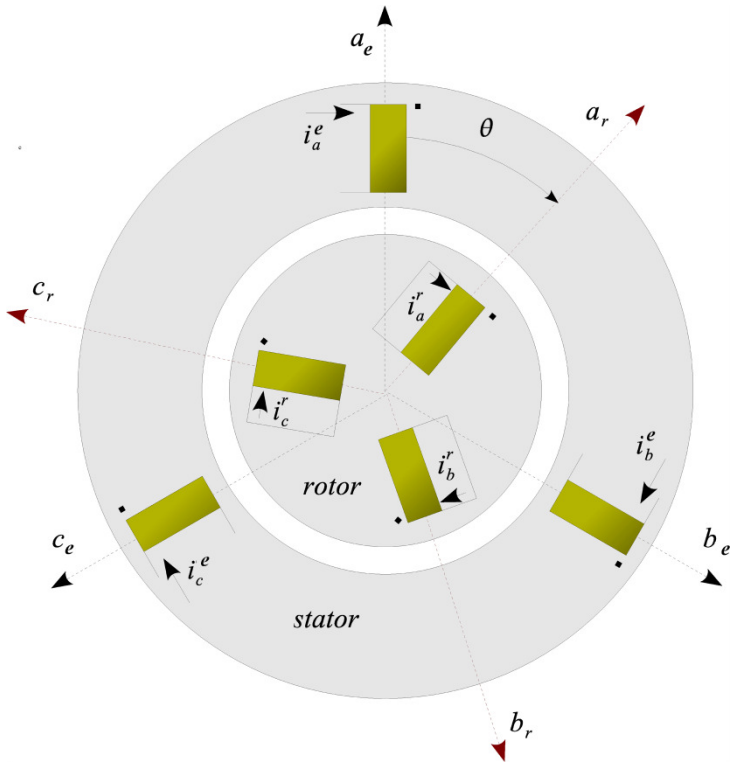


Figure 1: Induction Machine in "abc" coordinates frame

and $R_s, R_r$ are the stator and rotor resistances. $L_{\sigma s}, L_{\sigma r}$ are the leakage inductances. $L_{ms}, L_{mr}$ represent the magnetization inductances and $L_{sr}$ is the mutual inductance between stator and rotor windings. $J$ is the mechanical inertia, $\rho$ is the rotating friction, $T_m$ is the mechanical torque and $\theta$ is the angular rotor position referred to phase "$a$"in the stator coordinates frame. Expression 1 provides the flux linkage in each winding, by integrating $p[\lambda]$. Once, the flux linkage $[\lambda]$ is obtained in all the stator and rotor windings, it is possible to calculate the saturation coefficient for each inductance in $[L(\theta)]$ using the no load saturation test. Figure 2 shows the no load saturation test for an induction machine.

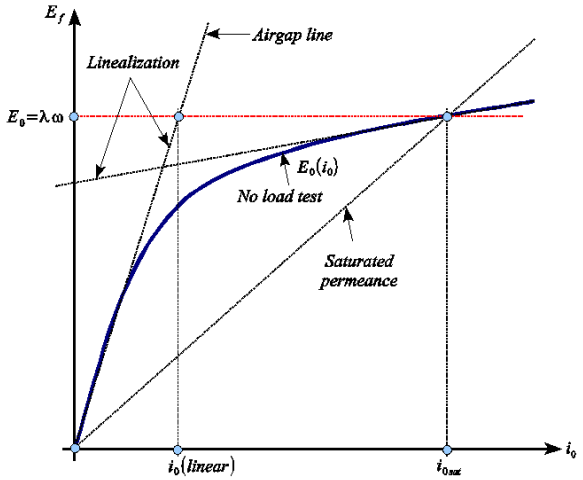


(a) No load saturation characteristic

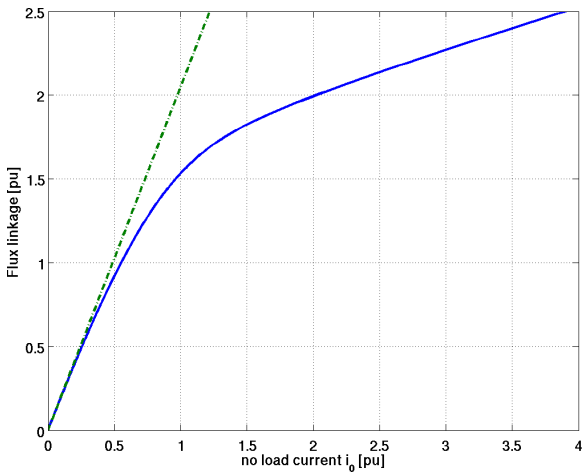


(b) No load saturation characteristic for the simulations

Figure 2: No load saturation test

Using the saturation curve shown in figure 2, the saturation coefficient can be obtained by dividing the no load current (required considering saturation) by the current in the linear case,

$$s = \frac{i_o(saturated)}{i_o(linear)} \tag{8}$$

As the flux leakage in any winding is different, there is a saturation coefficient for each one. The saturation coefficient affects only the magnetization inductances, the leakage inductances $L_{\sigma s}, L_{\sigma r}$ close their flux path throughout the air and their saturation is in practice negligible. Computing the mutual inductance between two different windings requires a special consideration. In this case the flux goes through two different paths, with its corresponding saturation coefficients. The mean value is a possible approximation, assuming the same flux paths for each winding,

$$S_{xy} = \frac{s_x + s_y}{2} \tag{9}$$

When the saturation coefficients $s_{as}$, $s_{bs}$, $s_{cs}$, $s_{ar}$, $s_{br}$ and $s_{cr}$ are obtained in the inductance matrix in (1) the inductances can be recalculated as,

$$[L_{ms}(sat)] = L_{ms}\begin{bmatrix} \frac{1}{s_{as}} & -\frac{1}{s_{as}+s_{bs}} & -\frac{1}{s_{as}+s_{cs}} \\ -\frac{1}{s_{bs}+s_{as}} & \frac{1}{s_{bs}} & -\frac{1}{s_{bs}+s_{cs}} \\ -\frac{1}{s_{cs}+s_{as}} & -\frac{1}{s_{cs}+s_{bs}} & \frac{1}{s_{cs}} \end{bmatrix} \tag{10}$$

$$[L_{mr}(sat)] = L_{mr}\begin{bmatrix} \frac{1}{s_{ar}} & -\frac{1}{s_{ar}+s_{br}} & -\frac{1}{s_{ar}+s_{cr}} \\ -\frac{1}{s_{br}+s_{ar}} & \frac{1}{s_{br}} & -\frac{1}{s_{br}+s_{cr}} \\ -\frac{1}{s_{cr}+s_{ar}} & -\frac{1}{s_{cr}+s_{br}} & \frac{1}{s_{cr}} \end{bmatrix} \tag{11}$$

$$[L_{sr}(\theta)] = 2L_{sr}\begin{bmatrix} \frac{\cos\theta}{s_{as}+s_{ar}} & \frac{\cos(\theta+2\pi/3)}{s_{as}+s_{br}} & \frac{\cos(\theta+4\pi/3)}{s_{as}+s_{cr}} \\ \frac{\cos(\theta+4\pi/3)}{s_{bs}+s_{ar}} & \frac{\cos\theta}{s_{bs}+s_{br}} & \frac{\cos(\theta+2\pi/3)}{s_{bs}+s_{cr}} \\ \frac{\cos(\theta+2\pi/3)}{s_{cs}+s_{ar}} & \frac{\cos(\theta+4\pi/3)}{s_{cs}+s_{br}} & \frac{\cos\theta}{s_{cs}+s_{cr}} \end{bmatrix} \tag{12}$$

## Simulation results

Three different simulation of the induction machine were developed in this work, a linear model (without saturation effect), the space vector model proposed by Tang [5] and the natural coordinates "*abc*" model corrected using the saturation coefficient proposed in this work. The linear model uses the airgap line shown in figure 2(a) in order to represent the magnetization characteristic, Tan's saturation model and the proposed method in this work. Figure 3 shows the simulation results (electric torque, angular speed and steady state currents) for the machine model without the saturation effect (linear model). Figure 4 shows the same results obtained taking into account the saturation characteristics shown in Fig. 2(b) using the Tang's saturation model [5]. In figure 5 are shown the results obtained considering the proposed method.

In Table I the linear model parameters used in the simulations and in the no load characteristic shown in figure 2(b) are presented. The no load characteristic is obtained by,

$$\begin{aligned} i_{msat} \;=\; & \frac{M_F - M_I}{\pi}\Big((\lambda-\Psi_T)\tan^{-1}(\tau_T(\lambda-\Psi_T)) - \Psi_T\tan^{-1}(\tau_T\Psi_T) + \cdots \\ & \cdots + \frac{1}{2\tau_T}\left[\log\left(1+(\tau_T\Psi_T)^2\right) - \log\left(1+\tau_T^2(\lambda-\Psi_T)^2\right)\right]\Big) + \frac{\lambda}{2}(M_F+M_I) \end{aligned} \tag{13}$$

where,

$$M_F = \frac{1}{L_{msat}} \;;\; \tau_T = \frac{\Theta_T L_{m0}}{\Psi_T L_{msat}} \;;\; M_I = \frac{\left(\frac{1}{L_{m0}} - M_F\left(1/2 - 1/\pi\tan^{-1}(\tau_T\Psi_T)\right)\right)}{1/2 + 1/\pi\tan^{-1}(\tau_T\Psi_T)} \tag{14}$$

Figures 3 and 4 shown a very similar behavior. Tang's model including saturation and the linear model has no effect in harmonic currents, dynamic performance or electric torque. There is only a small (≈25%) magnitude difference in the steady state currents, being the Tang's currents bigger than the obtained for the linear model. Nevertheless when the saturation coefficient in natural "*abc*" coordinates system is used to adjust the inductance according to the phase flux, a different dynamic and steady state performance is obtained as is shown in figure 5. The proposed model has similar magnitude for the currents than in Tang's model but it clearly includes the harmonic effect produced by the magnetic saturation characteristic.

Table I: Linear model parameters in per unit

| $R_s$ | $R_r$ | $L_{\sigma s}$ | $L_{\sigma r}$ | $L_m$ | $J = 2H\omega_s$ | $k_p$ | $V_{rms}$ | $f$ | $L_{m0}$ | $L_{msat}$ | $\Psi_T$ | $\Theta_T$ |
|---|---|---|---|---|---|---|---|---|---|---|---|---|
| 0.0324 | 0.066 | 0.2 | 0.2 | 2.0 | 150.8 | 1.0 | 1.0 | $60Hz$ | 2.05 | 0.23 | 1.8 | 1.0 |

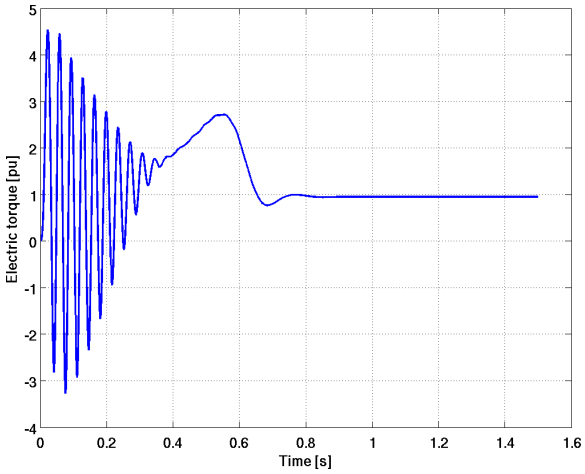


(a) Electric torque

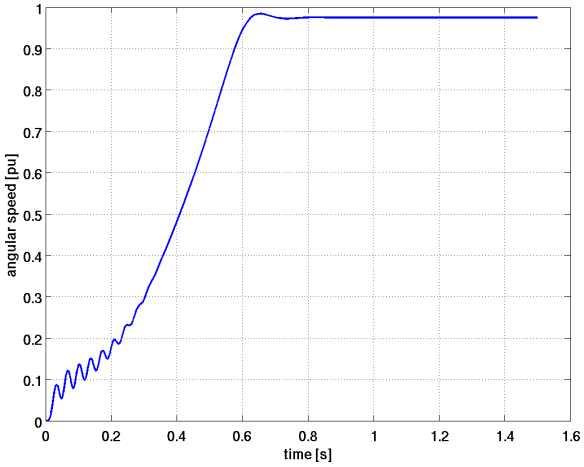


(b) Angular speed

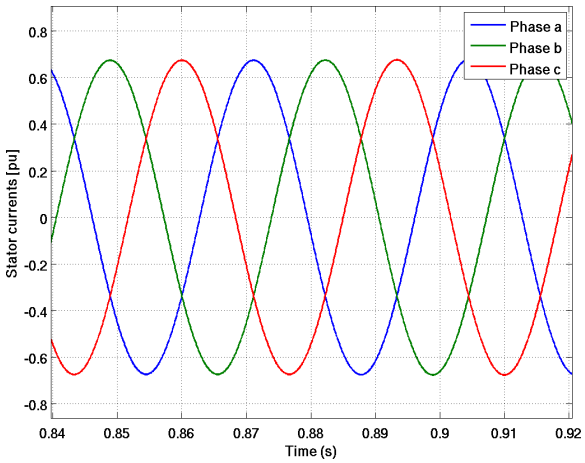


(c) Starting currents

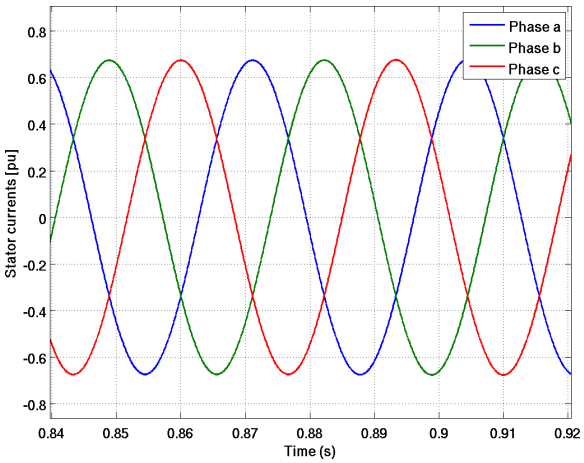


(d) Steady state currents

Figure 3: Results obtained with a lineal model (no saturation effect)

## Experimental Results

A wound rotor induction machine was experimentally tested at 110% of its rated voltage. The rated values of this machine are shown in Table II. The per unit parameters for the induction machine used in the experimental tests are shown in Table III. The experimental results presented in figure 6(a) show a similar harmonic content to the simulated ones presented in figure 6(b). The experimental and simulated

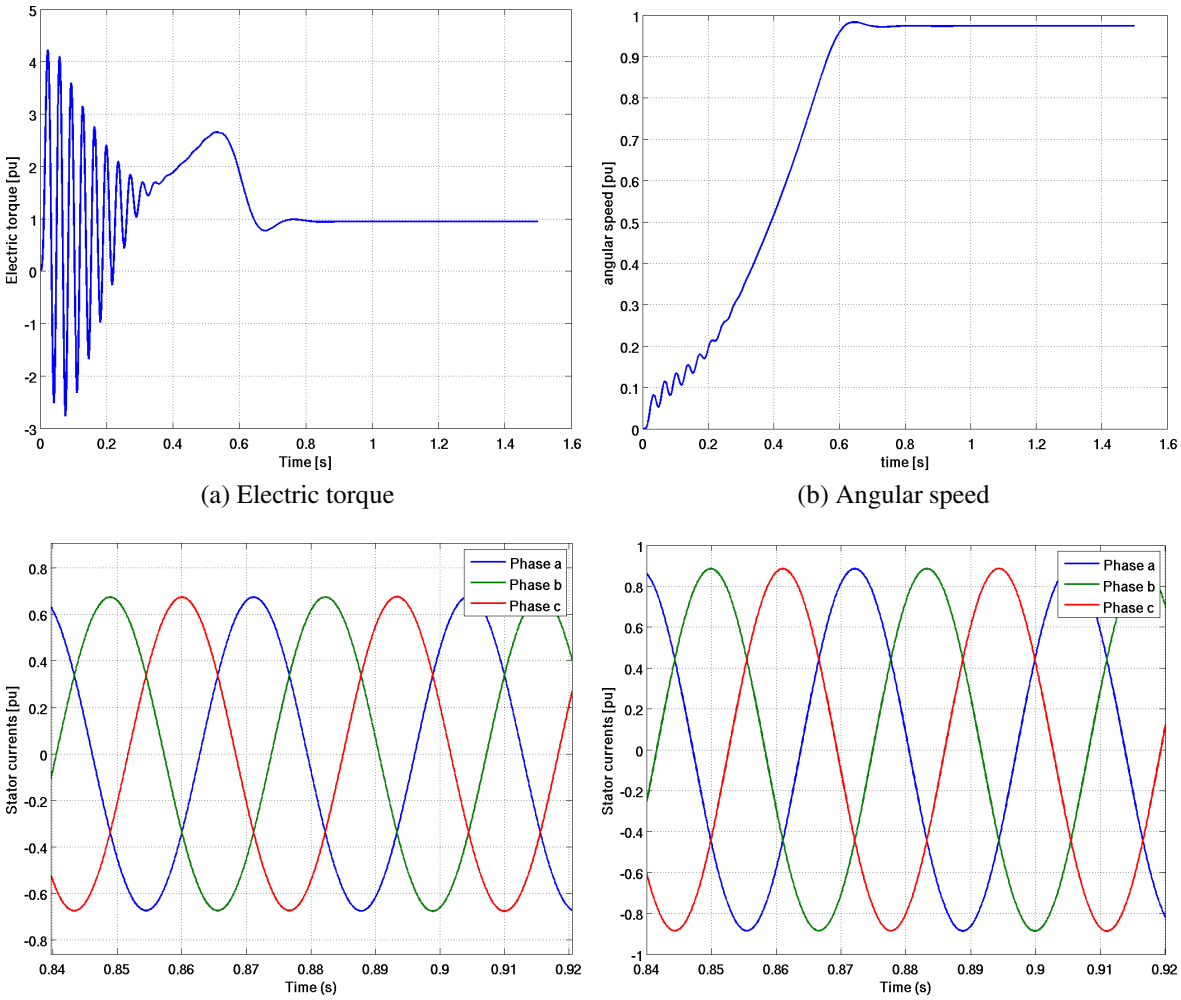


(a) Electric torque (b) Angular speed

(c) Starting currents (d) Steady state currents

Figure 4: Results obtained with Tang's model (saturated)

saturation characteristics are shown in Fig. 6(c). Considering that hysteresis in the magnetic path is not simulated, a close behaviour between the simulated and experimental results is obtained with the proposed model.

Table II: IM rated values.

| $V_n$ | $I_n$ | $P_n$ | $\cos\phi_n$ | $f_n$ | $n_n$ |
|---|---|---|---|---|---|
| $240/416V\ (\Delta - Y)$ | $16/9.2A$ | $4kW$ | 0.8 | $60Hz$ | $1710rpm$ |

Table III: Linear parameters in per unit for the experimental IM.

| $R_s$ | $R_r$ | $R_m$ | $X_m$ | $X_{\sigma s}$ | $X_{\sigma r}$ |
|---|---|---|---|---|---|
| 0.0327 | 0.066 | 11 | 1.2 | 0.0687 | 0.0772 |

## Conclusions

The reported models for operation under saturation of the induction machine use linear transformations that cannot be applied in nonlinear systems. A model that takes into acount the nonlinear saturation characteristic was presented and a comparison between the traditional and proposed methods shows the

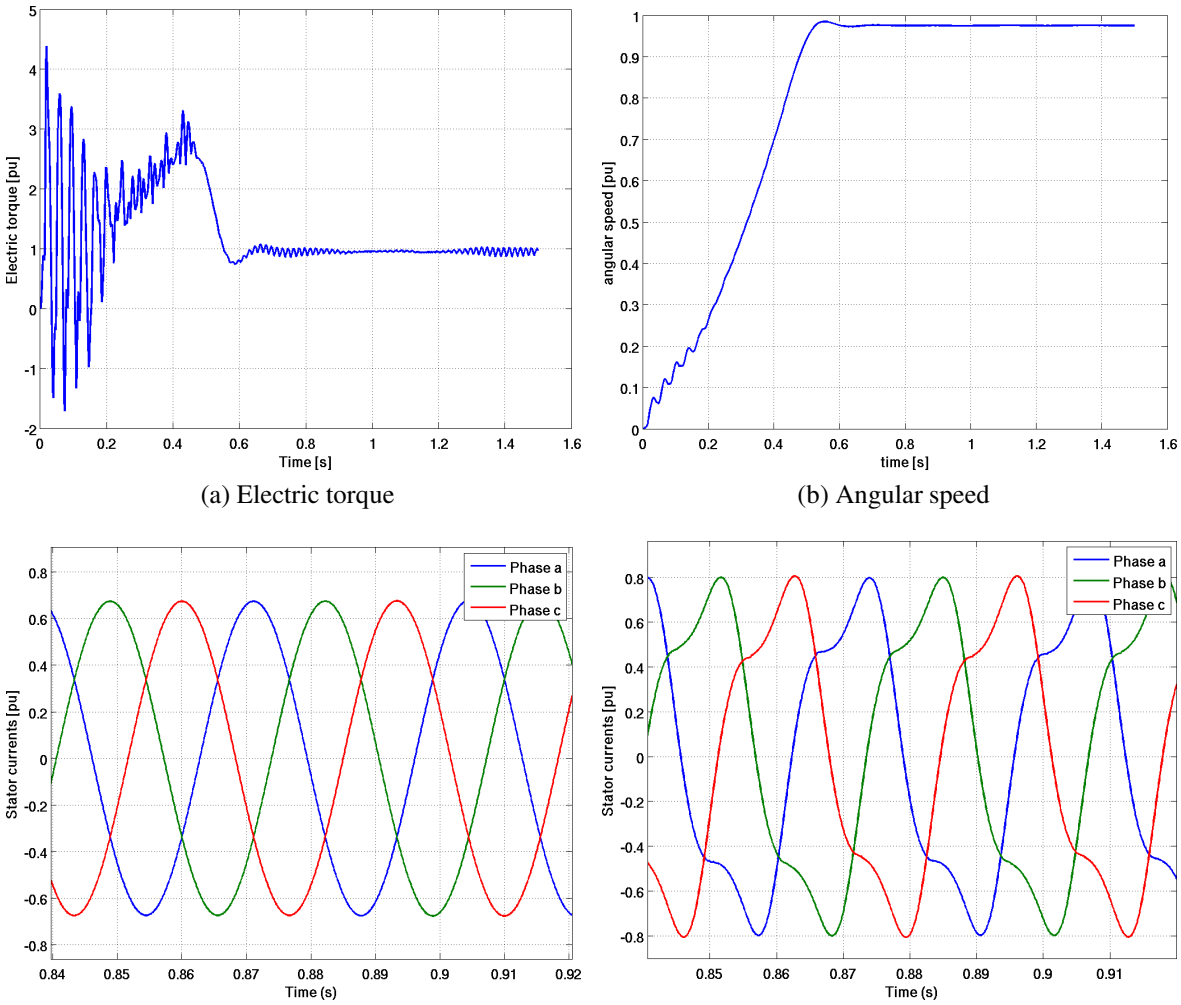


(a) Electric torque

(b) Angular speed

(c) Starting currents

(d) Steady state currents

Figure 5: Results obtained with proposed model (saturated)

advantages of considering the nonlinear effects in the inductance values.
The proposed method uses a permeance correction through a saturation coefficient for each magnetic path in natural coordinates “abc”. The results obtained with the proposed method show a more accurate stator current simulation under saturated operation. Experimental results are closer to the proposed method, and produce a better representation of stator currents.
The next step will be to verify the reported results using finite element methods because experimental results include the magnetic hysteresis phenomena and Eddy currents which introduce additional loading, shadowing the saturation effect.

# References

[1] Restrepo, J; Aller, J; Viola, J. C; Bueno, A; Guzmán, V; Gimenez, M. Switching Strategies for DTC on Asymmetric Converters, EPE JOURNAL. 2011. Vol. 21, pp. 35 - 42.

[2] Restrepo, J; Berzoy, Alberto; Ginart, Antonio; Aller, J; Harley, Ronald; Habetler, Thomas. Switching Strategies for Fault Tolerant Operation of Single DC-link Dual Converters. IEEE TRANSACTIONS ON POWER ELECTRONICS. 2012. Vol. 27, pp. 509 - 518.

[3] Brown, J.E.; Kovacs, K.P.; Vas, P.; , A Method of Including the Effects of Main Flux Path Saturation in the Generalized Equations of A.C. Machines, Power Apparatus and Systems, IEEE Transactions on , vol.PAS-102, no.1, pp.96-103, Jan. 1983

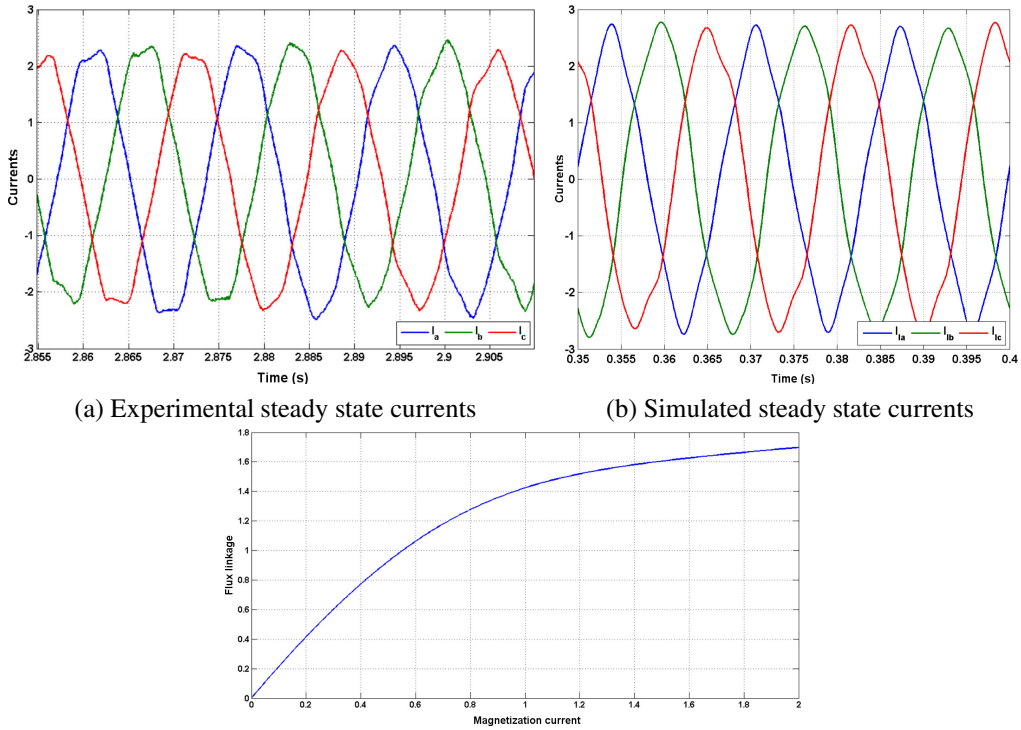


(a) Experimental steady state currents (b) Simulated steady state currents

(c) Experimental saturation characteristic

Figure 6: Comparisson between experimental and simulated steady state currents using the proposed model

[4] S. D. Pekarek, E. A. Walters, and B. T. Kuhn, An efficient and accurate method of representing magnetic saturation in physical-variable models of synchronous machines, IEEE Trans. Energy Convers., vol. 14, no. 1, pp. 72–79, Mar. 1999.

[5] Tang Ningping; Wu Hanguang; Qiu Peiji; A saturation model of induction machine by space vector, Electrical Machines and Systems, 2001. ICEMS 2001. Proceedings of the Fifth International Conference on , vol.1, no., pp.85-88 vol.1, 2001

[6] Liwei Wang; Jatskevich, J.; Including Magnetic Saturation in Voltage-Behind-Reactance Induction Machine Model for EMTP-Type Solution, Power Systems, IEEE Transactions on , vol.25, no.2, pp.975-987, May 2010

[7] Millán, Antonio; Villanueva, Carlos; Restrepo, J; Aller, J; Guzmán, V; Giménez, M; Viola, J. C. Comparing Parameter Identification Strategies for a Saturated Model of an Induction Motor . ANDESCON 2012. Cuenca, Ecuador. Noviembre 2012. pp. 1 - 4.

[8] IEEE Guide for Synchronous Generator Modeling Practices in Stability Analyses, IEEE Std 1110-1991 , pp.1, 1991.

[9] IEEE Guide: Test Procedures for Synchronous Machines Part I– Acceptance and Performance Testing Part II-Test Procedures and Parameter Determination for Dynamic Analysis, IEEE Std 115, pp.1-0, 2010.

[10] White, David C., and Herbert H. Woodson. Electromechanical energy conversion. Wiley, 1959.